Hagenmaier, H., Ebbighausen, W., Nicholson, G., & Votsch, W. (1970) *Z. Naturforsch., B: Anorg. Chem., Org. Chem., Biochem., Biophys., Biol. 25B*, 681-689.
Hantke, K., & Braun, V. (1973) *Eur. J. Biochem. 34*, 284-296.
Henderson, L. E., Oroszlan, S., & Konigsberg, W. (1979) *Anal. Biochem. 93*, 153-157.
Huang, Y. X., Ching, G., & Inouye, M. (1983) *J. Biol. Chem. 258*, 8139-8145.
Ichihara, S., Hussain, M., & Mizushiuma, S. (1981) *J. Biol. Chem. 256*, 3125-3129.
Inouye, S., Franceschini, T., Sato, M., Itakura, K., & Inouye, M. (1983) *EMBO J. 2*, 87-91.
Lai, J. S., Sarvas, M., Brammar, W. J., Neugebauer, K., & Wu, H. C. (1981) *Proc. Natl. Acad. Sci. U.S.A. 78*, 3506-3510.
McLaughlin, J. R., Murray, C. L., & Rabinowitz, J. C. (1981) *J. Biol. Chem. 256*, 11283-11291.
Michel, H. (1982) *J. Mol. Biol. 158*, 567-572.
Michel, H., Weyer, K. A., Gruenberg, H., & Lottspeich, F. (1985) *EMBO J. 4*, 1667-1672.
Michel, H., Weyer, K. A., Gruenberg, H., Dunger, I., Oesterhelt, d., & Lottspeich, F. (1986) *EMBO J. 5*, 1149-1158.
Nakamura, K., & Inouye, M. (1979) *Cell (Cambridge, Mass.) 18*, 1109-1117.
Nakamura, K., & Inouye, M. (1980) *Proc. Natl. Acad. Sci. U.S.A. 77*, 1369-1373.
Neugebauer, K., Sprengel, R., & Schaller, H. (1981) *Nucleic Acids Res. 11*, 2577-2588.
Ogata, R. T., Winters, C., & Levine, R. P. (1982) *J. Bacteriol. 151*, 819-827.
Ohashi, Y. (1984) *Biomed. Mass Spectrom. 11*, 383-385.
Okamura, M. Y., Feher, G., & Nelson, N. (1982) in *Photosynthesis* (Govindjee, Ed.) pp 195-274, Academic Press, New York.
Peterson, J. D., Nehrlich, S., Oyer, P. E., & Steiner, D. F. (1972) *J. Biol. Chem. 247*, 4866-4871.
Politt, S., Inouye, S., & Inouye, M. (1986) *J. Biol. Chem. 261*, 1835-1837.
Pugsley, A. P., Chapon, C., & Schwartz, M. (1986) *J. Bacteriol. 166*, 1083-1088.
Yamagata, H., Nakamura, K., & Inouye, M. (1981) *J. Biol. Chem. 256*, 2194-2198.
Yu, F., Inouye, S., & Inouye, M. (1986) *J. Biol. Chem. 261*, 2284-2288.

Dependence of the Activity of Beef Heart Mitochondrial Adenosinetriphosphatase on the Properties of the Catalytic Metal Ion†

Jeffrey L. Urbauer, Lonnie J. Dorgan, Thaddeus A. Tomaszek, Jr., and Sheldon M. Schuster*
Department of Chemistry and School of Biological Sciences, University of Nebraska, Lincoln, Nebraska 68588-0304
Received October 10, 1986; Revised Manuscript Received December 26, 1986

ABSTRACT: Several divalent metal ions were used as kinetic probes of the beef heart mitochondrial adenosinetriphosphatase (F_1) under a variety of conditions, and the relationship between the properties of the catalytic metal ion and the catalytic activity of the enzyme was examined. V_{max} for ATP hydrolysis was largest when metal ions characterized by intermediate values of acidity of coordinated water molecules (pK_a) and metal-nucleotide stability constants (K_{stab}) were present. As temperature increased, the peak of V_{max} vs. pK_a (or K_{stab}) shifted to lower initial values of pK_a or K_{stab}. The solvent deuterium isotope effect on V_{max} (^DV) was normal and largest when the metal ion present during F_1-catalyzed ATP hydrolysis was most acidic and the metal nucleotide stability constant was large. When an active site tyrosine on F_1 was nitrated, V_{max} was most affected when the metal ion present was least acidic and the metal nucleotide stability constant was small. The isotope effect on V/K ($^DV/K$) was normal, small, and apparently independent of the metal ion present. ADP inhibition of F_1-catalyzed ATP hydrolysis is competitive, and the K_i is independent of the metal ion present. The degree of P_i inhibition of F_1 is dependent on the metal ion present. The inhibition by P_i is competitive at low temperature and becomes noncompetitive as temperature increases. These and previous results support a mechanism whereby a water molecule coordinated to the metal ion of an enzyme-bound γ-monodentate metal-ATP complex is deprotonated to begin a series of events whereby a β,γ-bidentate metal-ATP complex is produced. Upon hydrolysis, the bond between the metal ion and the β-phosphate of ADP in the P_i-metal-ADP complex is broken before products (ADP and metal-P_i) are released.

The regulatory and catalytic mechanisms of beef heart mitochondrial ATPase (F_1)[1] have been extensively studied for many years. Several recent reviews discuss a wide variety of the regulatory and catalytic aspects of F_1 as well as the structure of this multisubunit complex (Cross, 1981; Pedersen, 1982; Amzel & Pedersen, 1983; Wang, 1983).

It has been shown that beef heart mitochondrial F_1 requires a divalent metal ion for catalytic activity and that any of several different ones will suffice. Furthermore, it has been shown that the rate of catalysis depends on the identity of the

† This work was supported by Grant PCM 84-09287 from the National Science Foundation.

[1] Abbreviations: ATPase, adenosinetriphosphatase; F_1, soluble beef heart mitochondrial ATPase; ATP, adenosine 5'-triphosphate; ADP, adenosine 5'-diphosphate; ATPβS, adenosine 5'-*O*-(2-thiotriphosphate); DCCD, dicyclohexylcarbodiimide; HEPES, *N*-(2-hydroxyethyl)-piperazine-*N*'-2-ethanesulfonic acid; tricine, *N*-[tris(hydroxymethyl)-methyl]glycine; P_i, inorganic phosphate; CHES, 2-(cyclohexylamino)-ethanesulfonic acid; HPLC, high-performance liquid chromatography; NBD-Cl, 7-chloro-4-nitro-2,1,3-benzoxadiazole.

0006-2960/87/0426-2914$01.50/0

metal ion (Pullman et al., 1960; Selwyn, 1967). It has been suggested that the size of the metal ion is important in determining the rate of F_1-catalyzed nucleotide hydrolysis (Selwyn, 1968; Adolfsen & Moudrianakis, 1978; Pedersen et al., 1974). Results of a recent study (Dorgan et al., 1984) indicate that temperature-sensitive metal-dependent parameters determine the extent to which different steps in the hydrolysis reaction regulate the reaction rate.

The results of the kinetic studies of Eigen, Hammes, and colleagues (Eigen & Hammes, 1960, 1961; Diebler et al., 1960; Hammes & Levison, 1964) lead to some very significant conclusions concerning the role of divalent metal ions in the association and dissociation of metal–nucleotide complexes and speculation concerning enzyme-catalyzed reactions in general which require divalent metal ions. Specifically, they indicate that the metals which would be most efficient in enzymatic catalysis involving ATP would be those with high acidity (ability to dissociate a proton from water in the primary coordination sphere) and those that favorably dissociate from metal–adenosine nucleotide complexes (low metal–nucleotide stability constant). Since for a single metal ion these two characteristics oppose each other, Mg^{2+}, Mn^{2+}, and Co^{2+} (medium in acidity and metal–nucleotide complex stability) would be more efficient catalytically than Ca^{2+} (favorable dissociation but low acidity) or Ni^{2+} (high acidity but unfavorable dissociation).

In this study, different metal ions were used to examine the participation of the metal ion in the F_1 catalytic process. The relationship between the properties of the catalytic metal ion, the catalytic process and rates, and the specific interaction of the metal ion with the enzyme and nucleotide substrates and products was studied. It has been proposed that initially F_1 binds a γ-monodentate metal–ATP complex as substrate and catalyzes conversion to a P_i–metal–ADP intermediate possibly via a discernable β,γ-bidentate metal–ATP complex (Bossard et al, 1980; Gruys et al., 1985). The results herein support the proposed metal nucleotide structures as well as define the contribution of the metal ion to the catalytic rate. The results also describe the interaction between an active site tyrosine, its acid–base catalytic properties (Esch & Allison, 1978), and the metal ion and metal–nucleotide complexes and conversion between these complexes. The results are consistent with the aforementioned proposals concerning metal ion properties and catalytic efficiency of ATP-utilizing enzymes.

Materials and Methods

General. ATP, ADP, D_2O (99.8%), citric acid, tetranitromethane, triethanolamine hydrochloride, tricine, HEPES, and CHES were all purchased from Sigma Chemical Co. [^{32}P]P_i (carrier free) was purchased from Amersham. The metal salts (chlorides) and other reagents were from common commercial sources and were of analytical purity.

Beef Heart Mitochondrial ATPase (F_1). F_1 was isolated and purified by either the method of Spitsberg and Blair (1977) or a modified form of the method of Knowles and Penefsky (1972) as indicated. The modification of the latter method consisted of an extra centrifugation step (90 min at 30 000 rpm) after the overnight incubation at pH 9.2. The supernatant fluid was discarded and the pellet resuspended with a homogenizer in the same buffer. All succeeding steps were as described. This extra centrifugation step results in a more homogeneous enzyme preparation as shown by the elution profile of the enzyme upon HPLC size exclusion chromatography (Gruys and Schuster, unpublished results). Protein concentrations were determined by the biuret method (Layne, 1957), the method of Lowry et al. (1951), or that of Bradford (1976) using the Bio-Rad protein assay concentrate.

Nitration and Temperature Studies. F_1 was isolated by the method of Spitsberg and Blair (1977). Experiments were conducted in a total volume of 1.0 mL containing 25 mM triethanolamine hydrochloride, 20 mM sodium bicarbonate, and varying concentrations of ATP, pH 8.0. The concentration of the metal cation was maintained at a 0.1 mM excess over ATP. The temperature was 30 °C for the nitration studies and was as indicated for the results in Figure 2. Nitration of F_1 was performed as described previously (Dorgan & Schuster, 1981). The hydrolysis reaction was initiated by addition of F_1 and terminated after 40 s (which was determined to be well within the linear range of product formation) by addition of 0.5 mL of 10% sodium dodecyl sulfate. Analysis of phosphate concentration was performed as described by Petersen (1978). To avoid differences in phosphate concentrations due to acid-catalyzed hydrolysis of ATP, the length of time between addition of the assay reagents and absorbance readings was equal for all samples. Kinetic constants were determined from the slopes and intercepts of weighted least-squares lines through Lineweaver–Burk plots.

Isotope Effect Studies. F_1 was isolated by the method of Knowles and Penefsky (1972) modified as discussed above. Before use, the F_1/ammonium sulfate suspension was centrifuged and the F_1 was resuspended in a solution of 25 mM HEPES and 25 mM CHES in either H_2O or D_2O at the appropriate pH(D). It was determined that incubation of the F_1 in D_2O as opposed to H_2O over the time course of the experiments did not affect the activity of the F_1. In all cases the temperature was maintained at 30 °C.

Measurements of the kinetic isotope effects on V_{max} and V_{max}/K_m (V/K) were made at equivalent pH(D) (Schowen & Schowen, 1982). To determine the appropriate pH(D), the velocities of the F_1-catalyzed ATP hydrolysis reactions in the presence of either Mg^{2+}, Ni^{2+}, or Ca^{2+} in H_2O or D_2O (99.8%) were measured from pH(D) 7.0 to pH(D) 10.0 at intervals of 0.25 pH(D) unit. When D_2O was present, the pH meter reading was adjusted according to the equation of Salomaa et al. (1964). For these experiments, the concentration of metal–ATP was 1.0 mM and the concentration of free metal was maintained constant over the entire pH(D) range. Stability constants for the various metal–ATP complexes were from Taqui Khan and Martell (1966). The values used for pK_a were 6.95 and 7.48 in H_2O and D_2O, respectively. Reactions were performed in a total volume of 1.0 mL, buffered by 25 mM HEPES/KOH and 25 mM CHES/KOH. Velocities were assessed by measuring production of phosphate by using a modified form of the assay for inorganic phosphate as described by Heinonen and Lahti (1981). Reactions were started by addition of F_1 and terminated after 1.0 min (within the linear range of product formation) by addition of 2.0 mL of the AAM solution (3 parts acetone, 1 part 10.0 N H_2SO_4, 1 part 15.0 mM ammonium molybdate). One minute after AAM addition, 200 μL of 1.0 M citric acid was added to complex excess molybdate to eliminate further color development by phosphate produced from acid-catalyzed ATP hydrolysis. Absorbance was measured at 355 nm. By use of this assay, absorbance is linear with phosphate concentration from 5 to over 400 nmol (per milliliter) of phosphate. Acid-washed glassware was used in all cases.

Once equivalent pH(D) values were found for ATP hydrolysis catalyzed by F_1 in the presence of each of the three metal ions used in these studies (Mg^{2+}, Ca^{2+}, and Ni^{2+}), the velocities of the F_1-catalyzed Mg–ATP, Ca–ATP, and Ni–ATP hydrolysis reactions were measured in either H_2O or D_2O

at the appropriate pH(D). For these reactions, the concentration of metal–ATP was varied from 0.05 to 1.0 mM, while concentration of free metal was held constant. Stability constants and values of pK_a were as mentioned above. Reactions were started and stopped and velocities determined as described above for the experiments to determine equivalent pH(D).

Because of the apparent cooperativity observed during ATP hydrolysis catalyzed by F_1, the double-reciprocal plots of the data are nonlinear. The data were fitted to the equation for a hyperbola curved near the $1/v$ axis and becoming tangent to one asymptote at high $1/v$ values (Cleland, 1967). Fitting was accomplished by the least-squares minimization algorithm of Fletcher and Powell (1963). Estimation of the standard deviations in the parameters were obtained from the variance–covariance matrix (Draper & Smith, 1966).

Nomenclature. Nomenclature for isotope effects is that of Northrop (1981a,b, 1982). For example, the isotope effect on V_{max}, $V_{max}(H_2O)/V_{max}(D_2O)$, is represented ^DV. That for the isotope effect on V/K is $^DV/K$. The intrinsic isotope effect, that for the isotopically sensitive rate constant, is represented as ^Dk [$k_f(H_2O)/k_f(D_2O)$, where subscript f stands for forward; subscript r would analogously stand for reverse]. Finally, $^DK_{eq} = {}^Dk_f/{}^Dk_r$.

Similar nomenclature is used for nitration effects. For example, ^NV is the nitration effect on V_{max}, $V_{max}(U)/V_{max}(N)$ (where U stands for unnitrated enzyme and N stands for nitrated enzyme). Similarly, $^Nk = k_f(U)/k_f(N)$, and $^NK_{eq} = {}^Nk_f/{}^Nk_r$.

Values represented as C_r (reverse commitment to catalysis) and R_f/E_f (ratio of catalysis divided by the equilibration preceding catalysis) are defined by Northrop (1981a,b; 1982).

ADP Inhibition Experiments. F_1 was isolated by the method of Knowles and Penefsy (1972) modified as described above. In these experiments, ADP was tested as an inhibitor of Ca–ATP, Mn–ATP, Mg–ATP, and Ni–ATP hydrolyses. The concentration ATP was varied from 0.05 to 1.0 mM, and equimolar metal chloride was present. The concentrations of added ADP used were 30.0, 60.0, and 120.0 μM. The experiments were performed in a total volume of 1.0 mL containing 50.0 mM tricine and 20.0 mM sodium bicarbonate, at a final pH of 8.0. The reactions were initiated by addition of F_1 and terminated after 1 min. Reactions were terminated, and phosphate production was measured as described above for the isotope effect studies. Values of K_i were obtained from replots of Lineweaver–Burk plots using a weighted least-squares procedure weighted on the basis of the inverse variances of the slopes of the lines in the Liveweaver–Burk plots. Error limits were obtained from standard error of estimate values of slope and y intercept of the replots.

P_i Inhibition Experiments. F_1 was isolated by the method of Spitsberg and Blair (1977). In these experiments, P_i was tested as an inhibitor at ATP hydrolysis catalyzed by F_1 in the presence of various metal ions at 20 and 30 °C. The concentration of ATP was varied from 0.25 to 2.0 mM, and equimolar metal chloride was present. The concentrations of added P_i used were 5.0, 10.0, and 20.0 mM. The experiments were performed in a total volume of 1.0 mL containing 50.0 mM tricine, pH 8.0. Velocities were determined by measuring ^{32}P released as $^{32}P_i$. A small carrier amount of [^{32}P]ATP [prepared by the method of Schendel and Wells (1973)] was added to each reaction mixture. Reactions were started by addition of F_1. The reactions were terminated within the linear range of product formation, and [^{32}P]P_i was separated from the reaction mixture and unreacted [^{32}P]ATP by the extraction method of Pullman (1967). After the two phases separated, 1.0 mL of the organic phase (which contained the free ^{32}P) was added to scintillation fluid and the radioactivity measured. The kinetic constants were obtained by least-squares fits to the Michaelis–Menten equation and slope and intercept replots of the data.

Table I: Maximal Rates of Metal–ATP Hydrolysis Catalyzed by F_1, pK_a Values for Metal-Coordinated Water Molecules, and Metal–Nucleotide Stability Constants for Several Divalent Metal Ions

divalent metal ion	k_{cat}[a] (s^{-1})	$pK_a(H_2O)$[b]	log stability constants ATP[c]	ADP[d]	AMP[d]
Ba^{2+}	0	13.5	3.29	2.36	1.73
Sr^{2+}	0	13.3	3.54	2.54	1.79
Ca^{2+}	71	12.9	3.97	2.86	1.85
Mg^{2+}	624	11.4	4.22	3.17	1.97
Mn^{2+}	720	10.6	4.78	4.16	2.40
Co^{2+}	379	10.2	4.66	4.20	2.53
Cd^{2+}	318	10.1	[e]	[e]	[e]
Ni^{2+}	95	9.9	5.02	4.50	2.84
Zn^{2+}	269	9.0	4.85	4.28	2.72
Cu^{2+}	7.5	8.0	6.13	5.90	3.18

[a] From Dorgan et al. (1984). [b] From Baes amd Mesmer (1976). [c] From Taqui Kahn and Martell (1966). [d] From Taqui Kahn and Martell (1967). [e] Not available from above references.

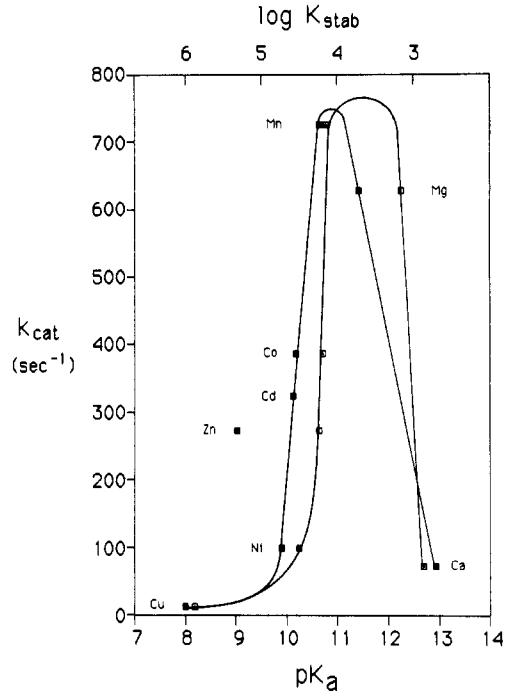

FIGURE 1: Maximal rates of F_1-catalyzed hydrolysis of ATP vs. the pK_a (■) of water coordinated to the metal ion present and vs. the stability constant (□) of the particular metal–ADP complex.

RESULTS

Recently, the efficiency of several divalent metal ions to support ATP and ITP hydrolyses catalyzed by F_1 was explored (Dorgan et al., 1984). The maximal rates of ATP hydrolysis catalyzed by F_1 in the presence of these divalent metal ions are summarized in Table I. As shown, rates of F_1-catalyzed Mg–ATP and Mn–ATP hydrolyses are about twice those of Cd–ATP, Co–ATP, and Zn–ATP hydrolyses and are more than 6 times greater than the rates of Ca–ATP and Ni–ATP hydrolyses.

Also shown in Table I are values of the first pK_a for a water molecule in the primary coordination sphere for several divalent metal ions, as are values of the stability constants

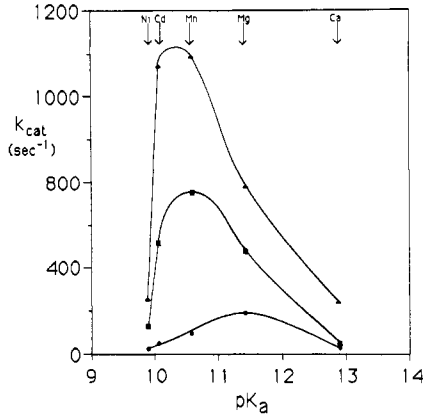

FIGURE 2: Effect of temperature on the maximal rate of F_1-catalyzed ATP hydrolysis vs. the pK_a of the water coordinated to the metal ion present. Temperatures are 10 (●), 30 (■), and 50 °C (▲). Metal ions used are (from left to right) Ni^{2+}, Cd^{2+}, Mn^{2+}, Mg^{2+}, and Ca^{2+}.

(expressed as logarithms) for complexes of these metal ions formed with ATP, ADP, and AMP. As seen in Figure 1, a plot of the maximum velocity (reported as k_{cat}, assuming a molecular weight of 360 000 for F_1) vs. the pK_a of the metal-coordinated water is a smooth curve (with the exception of Zn^{2+}) with an optimum centered around a pK_a of about 11. If these velocities were plotted vs. the stability constants of metal–ADP complexes, the curve would be similarly shaped (with Zn^{2+} now on the curve). These results are in accord with the suggestions of Hammes and Levison (1964) as to the efficiency of these different metal ions to promote F_1-catalyzed ATP hydrolysis (see the introduction).

Temperature Dependence of Metal–ATPase Activity. Experiments were conducted to explore the dependence on temperature of F_1-catalyzed ATP hydrolysis activity using different metal ions to support hydrolysis. Figure 2 shows the results of these experiments. As seen in Figure 2, as the temperature increased, the maximum velocity (reported as k_{cat}) of F_1-catalyzed ATP hydrolysis increased regardless of which divalent metal ion was present. However, as the temperature increased, the optimum in the curve of k_{cat} vs. the pK_a of metal-coordinated water molecules (or metal–nucleotide stability constants) shifted toward lower initial pK_a values and higher initial metal–nucleotide stability constants. These pK_a and K_{stab} values are referred to as initial because as temperature is changed, these values change. The relationship between the observed temperature dependence of these velocities and the metal-dependent parameters will be examined (see Discussion).

Metal Dependence of Solvent Isotope Effects. A series of experiments was performed to determine the equivalent pH(D)s for F_1-catalyzed ATP hydrolysis in the presence of either Ca^{2+}, Mg^{2+}, or Ni^{2+}. Over the pH(D) range of 7.0–10.0, the optimum values of pH were 8.25, 8.0, and 8.0 for Ca^{2+}, Mg^{2+}, and Ni^{2+}, respectively, while the optimum values of pD were 8.5, 7.75, and 7.75, respectively. In all cases, near the optimum, the curves of velocity vs. pH(D) were relatively flat, so the velocities were relatively pH(D) independent near the optima. In all instances, the experiments to determine the isotope effects were performed at the optimum pH(D).

Figure 3 shows Lineweaver–Burk plots of the data and the lines calculated from the fit to the data as described under Materials and Methods. The overall fit was very good, as the sums of squares of the residuals ranged from 2.08×10^{-3} to 1.8×10^{-5} for 12 to 15 data points per set. Also, the average percent deviation or residuals from observed values for any particular data set ranged from only 1.5% to 5.2%. Importantly, the negative cooperativity present during F_1-catalyzed Mg–ATP hydrolysis [originally shown to occur by Ebel and Lardy (1975)] is also seen when Ni^{2+} is the metal ion present. However, during Ca–ATP hydrolysis, positive cooperativity is observed.

Table II: Isotope Effects on F_1-Catalyzed ATP Hydrolysis in the Presence of Different Divalent Metal Ions

[metal–ATP^{2-}] (mM)	^Dv		
	Ni^{2+}	Mg^{2+}	Ca^{2+}
∞[a]	2.04 ± 0.54	1.91 ± 0.77	1.04 ± 0.14
1.0	1.60 ± 0.014 (1.55)[b]	1.41 ± 0.014 (1.51)	1.12 ± 0.01 (1.08)
0.1	1.26 ± 0.033 (1.32)	1.27 ± 0.043 (1.24)	1.22 ± 0.03 (1.20)

[a] The values at [metal–ATP^{-2}] = ∞ were calculated by extrapolation using parameters calculated from the fitted data (see Materials and Methods). At [substrate] = ∞, ^Dv = ^DV(apparent) or ^DV at a single concentration of the other substrate, in this case H_2O or D_2O. [b] The values in parantheses are calculated from parameters obtained from the fit of the data as described under Materials and Methods.

Table III: Dependence of the Activity of Nitrated F_1 on the Metal Ion Present during ATP Hydrolysis: Percent Activity Remaining after Nitration[a]

divalent metal ion		
Ca^{2+}	Mg^{2+}	Ni^{2+}
54.5	72.1	91.6

[a] An average of three residues per F_1 molecule were nitrated.

The observed values of the isotope effect at various substrate concentrations are shown in Table II, along with values calculated from velocities obtained from the fitted parameters (to the right of the slash). At high substrate concentrations, the values of ^Dv when Ni^{2+} and Mg^{2+} are present are much higher than when Ca^{2+} is used, and all are significantly different from one another. At low [S], the values of ^Dv when Ni^{2+} and Mg^{2+} are present are much lower than at high [S] and that for Ca^{2+} is higher. The values calculated from the fitted parameters also decrease with decreasing [S] when Ni^{2+} and Mg^{2+} are present and increase when Ca^{2+} is present.

Extrapolation to infinite substrate concentration reveals a normal isotope effect on V_{max}) [$^DV_{app}$ or ^DV at a single H_2O or D_2O concentration, nomenclature of Northrop (1981a)], as the data for ^Dv suggest, when Ni^{2+} or Mg^{2+} is present and none when Ca^{2+} is present. Unfortunately, the error in ratios of V_{max}/K_m was too great in all cases to produce significant values of $^DV/K$. However, the values of ^Dv suggest a small normal isotope effect on V/K, the magnitude of which is independent of the identity of the metal ion present.

Metal Dependence of Activity of Nitrated F_1. Table III shows results of experiments that measured Ca-ATPase, Mg-ATPase, and Ni-ATPase activities catalyzed by nitrated F_1 and F_1 that had not been nitrated. In all cases, the maximum velocities were lower during catalysis by nitrated F_1. As seen in Table III, Ca-ATPase activity was most affected by nitration, Ni-ATPase activity was least affected, and the effect on Mg-ATPase activity was intermediate.

Nitration of tyrosine residues makes the phenolic group more acidic or less efficient as a base. This is analogous to deuterium isotope effects since deprotonation during catalysis is more difficult with deuterium, or in other words, the basic group responsible is not effective when deuterium is present. The relationship between these effects and F_1 catalysis will be examined (see Discussion).

Metal Dependence of ADP Inhibition. In Table IV are shown the K_i values for ADP inhibition of F_1-catalyzed ATP

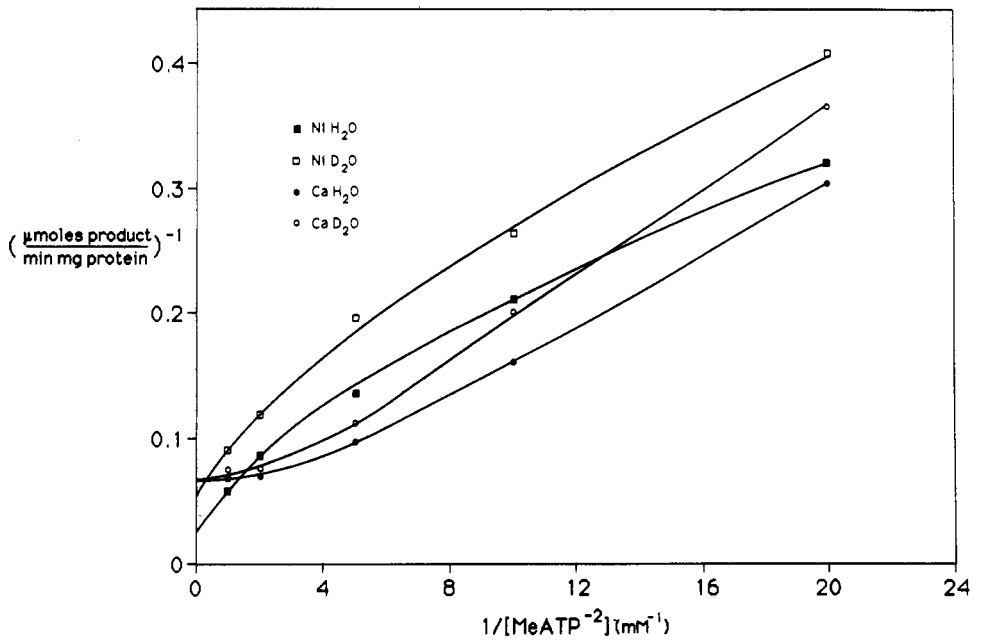

FIGURE 3: Lineweaver–Burk plots of F_1-catalyzed Ni–ATP or Ca–ATP hydrolysis in either H_2O or D_2O. Points represent data as averages of several determinations at each concentration, and lines are those calculated from the fit of the data as described under Materials and Methods. Points for Mg–ATP hydrolysis are not shown.

Table IV: Values of K_i for ADP Inhibition of F_1-Catalyzed ATP Hydrolysis in the Presence of Either of Several Divalent Metal Ions

divalent metal ion	K_i (mM)	divalent metal ion	K_i (mM)
Ca^{2+}	97 ± 18	Mn^{2+}	73 ± 14
Mg^{2+}	79 ± 8	Ni^{2+}	77 ± 10

hydrolysis in the presence of either Ca^{2+}, Mg^{2+}, Mn^{2+}, or Ni^{2+}. It has been shown that ADP is a competitive inhibitor of ATP hydrolysis catalyzed by F_1 when Mg^{2+} is the divalent metal ion present (Pedersen, 1975). Although not shown, the inhibition pattern remains competitive when either Ca^{2+}, Mn^{2+}, or Ni^{2+} is present.

Also, it has been shown that ADP binding to F_1 is independent of the presence of a metal ion (Senior, 1973). If this is the case, the degree of inhibition of F_1 by ADP should be the same regardless of the metal ion used to support hydrolysis. Table IV shows the K_i value for ADP hydrolysis is not changed by the metal ion used to support hydrolysis. This suggests that products are released from the enzyme after the metal–ADP bond is broken.

Metal and Temperature Dependence of P_i Inhibition. It has been shown that inorganic phosphate (P_i) is an inhibitor of rat liver F_1-catalyzed Mg-ATPase activity (Ebel & Lardy, 1975). The results of experiments to explore the inhibition of F_1-catalyzed ATP hydrolysis by P_i in the presence of several different metal ions at different temperatures are shown in Table V. The results show that as temperature increases, P_i inhibition of F_1-catalyzed ATP hydrolysis in the presence of either Ni^{2+}, Cu^{2+}, Cd^{2+}, or Mg^{2+} changes from competitive to noncompetitive. When Mn^{2+} was present, there was no apparent inhibition by P_i at the low temperature, but as the temperature increased, P_i became a competitive inhibitor. P_i inhibition with Ca^{2+} present could not be explored because of the high concentration of P_i needed to inhibit F_1 and the low value of K_{sp} for calcium phosphate.

In contrast to the results seen for ADP inhibition of ATP hydrolysis, P_i inhibition of F_1 was dependent on the metal ion present. The results are shown in Table V. In general, when the metal present forms a tight complex with P_i (Cu^{2+}, Ni^{2+}, Cd^{2+}, Co^{2+}), inhibition is greater than when the complex has a low K_{stab} (Mg^{2+}, Mn^{2+}). This is expected on the basis of the results of Penefsky (1977) and Younis et al. (1983), which show that P_i binding is dependent on the presence of a metal ion.

Table V: Values of K_i for P_i Inhibition of F_1-Catalyzed ATP Hydrolysis in the Presence of Either of Several Divalent Metal Ions at Two Temperatures

	20 °C	30 °C	
divalent metal ion	K_i (mM)	K_{is} (mM)	K_{ii} (mM)
Cu^{2+}	11.4	8.6	32.1
Ni^{2+}	9.3	5.5	12.9
Cd^{2+}	10.7	11.6	21.5
Co^{2+}	10.1	*a*	*a*
Mn^{2+}	ND[b]	38.2	*c*
Mg^{2+}	55.1	63.6	178

[a] These values were not determined. [b] ND, not detectable. [c] Competitive inhibition.

Results of Simulations. Table VI presents results of simulations of the metal dependence of the isotope effects on F_1-catalyzed metal–nucleotide hydrolysis and metal dependence of the velocity of the reaction. The mechanism presented in Figure 4 (see Discussion) is used as the basis for the simulations.

The rate constants for the individual steps of the mechanism in Figure 4 are also presented in that figure. The values are reasonable on the basis of other published rate constants and equilibrium constants whether measured or expected (Dorgan et al., 1984; Gresser et al., 1982).

The rate constants k_1–k_4 describe reversible substrate binding, the substrates being H_2O and γ-monodentate metal–ATP (see Discussion). These values are reasonable under conditions of high substrate concentration (Gresser et al., 1982; Dorgan et al., 1984). In the scheme presented, H_2O binds first and metal–ATP second, although this order may be reversed or random as discussed below.

The rate constants k_5–k_8 describe precatalytic equilibration steps. These are necessary to account for the full uncertainty expressed in the equation for calculating R_f/E_f (ratio of catalysis to equilibration preceding catalysis; Northrop, 1981a,b) in the expression for ^DV.

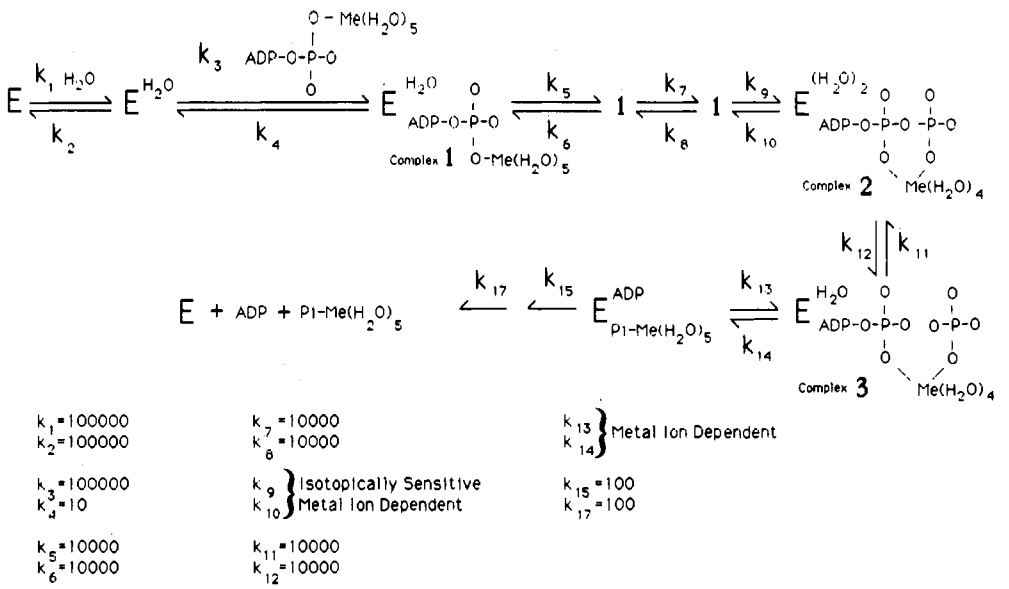

FIGURE 4: A mechanism for hydrolysis of ATP catalyzed by F_1. Description of rate constant values appears under Results. The scheme is not intended to describe the specific interactions of active site amino acid residues and the metal ion or nucleotide. As such, metal ion ligands other than nucleotide phosphate oxygens are simply designated as water molecules, and no charges appear on nucleotide phosphate oxygens.

Table VI: Simulations of the Metal Ion Dependence of the Isotope Effects and Maximum Velocity of F_1-Catalyzed ATP Hydrolysis[a]

row	Ca^{2+}		Mg^{2+}		Ni^{2+}	
1	1000	4000	500	1000	200	200
	10000	100	10	50	0.666	20
	0.1	40	50	20	300	10
	1.00	23.6	1.81	33.9	2.26	21.1
2	1000	2500	500	500	200	200
	10000	50	10	25	2	20
	0.1	50	50	20	100	10
	0.96	21.9	1.76	31.7	2.26	21.0
3			500	1000	300	200
			25	50	3	20
			20	20	100	10
			1.8	33.7	1.94	23.5
4	200	500	500	500	200	50
	2000	10	50	50	0.666	5
	0.1	50	10	10	300	10
	1.13	9.19	1.70	30.0	1.77	12.88
5	300	500			100	50
	3000	10			0.333	5
	0.1	50			300	10
	0.94	9.64			2.29	10.79
6	300	1000			100	100
	3000	20			0.333	10
	0.1	50			300	10
	1.19	13.9			2.65	13.8

[a] Values in columns are arranged as follows:

k_9	k_{13}
k_{10}	k_{14}
ratio k_9/k_{10}	ratio k_{13}/k_{14}
${}^{D}V$	V_{max}

k_9/k_{10} represents the isotopically sensitive step which is formation of a β,γ-bidentate metal–ATP complex from a γ-monodentate complex. The values of the rate constants will depend on the metal ion because the enzyme first must deprotonate a metal-coordinated H_2O molecule, and the values of pK_a for these water molecules are different for different metal ions (see Discussion). The mono- to bidentate equilibrium following (or concomitant with) proton removal would also be metal dependent.

k_{11}/k_{12} represents nucleotide hydrolysis, which, according to Gresser et al. (1982) has an equilibrium constant of 1.0.

k_{13}/k_{14} represents association–dissociation of the metal–ADP bond. These rate constants also depend on the metal ion present since the stability constants for the different metal–ADP complexes are different.

k_{15} and k_{17} represent product release. These steps are presumed to be slow (Gresser et al., 1982). The scheme makes no distinction as to the order of product release, as will be discussed later. However, it is unlikely that the metal ion leaves with ADP (see Discussion).

The simulated values of ${}^{D}V$ presented in Table VI were calculated by using the method and equations described by Northrop (1981a,b, 1982) as were values of ${}^{D}V/K$ (not shown). Values of ${}^{D}V$ and ${}^{D}V/K$ were also calculated from the rate equations for the mechanism presented in Figure 4, by calculating V_{max} and V/K according to the method of net rate constants as described by Cleland (1975). Complete agreement was obtained for values of the isotope effects calculated by these two methods. The value of ${}^{D}K_{eq}$ was 0.33 (Schowen, 1977), and the value of ${}^{D}k$ was chosen to be 5.0.

Values of ${}^{D}V$ and V_{max} are calculated for a number of sets of the rate constants k_9, k_{10}, k_{13}, and k_{14}, and the results are shown in Table VI. All other rate constants, for the results presented in Table VI, are held constant, the values for these appearing in Figure 4.

The results are arranged in three columns labeled Ca^{2+}, Mg^{2+}, and Ni^{2+}. The values of the rate constants in a particular column were chosen such that the ratios k_9/k_{10} and k_{13}/k_{14} parallel the values of pK_a for the metal ion and K_{stab} for the metal–nucleotide stability constant relative to the other metal ions. For example, the ratio $K_{stab}(Mg)/K_{stab}(Ni)$ is approximately 2, and the ratio of $(k_{13}/k_{14})_{Mg\text{-}ADP}/(k_{13}/k_{14})_{Ni\text{-}ADP}$ for the values in Table VI is approximately 2. In some cases these ratios are varied to illustrate the effects of these changes on the calculated values of isotope effects and V_{max}'s.

The absolute values of the rate constants were also chosen in accordance with the properties of the metal ions. In general, Ca^{2+} exchanges ligands much faster than does Mg^{2+} or Ni^{2+} (Basolo & Pearsen, 1967; Hammes & Levison, 1964). Thus, the values of the rate constants k_9, k_{10}, k_{13}, and k_{14} in Table

VI are generally much larger for Ca^{2+} than for Mg^{2+} or Ni^{2+} in rows 1–3. This is not necessarily the case for rows 4–6. Rows 4–6 demonstrate that these rate constants need not be vastly different depending on the metal ion present in order to simulate the observed isotope effects, since on the enzyme the values may be much more similar to one another.

As indicated above concerning the results of the similations of Table VI, the values of the rate constants were chosen to attempt to describe how different metal ions affect the F_1 mechanism in a manner consistent with the properties of the metal ions. Most importantly, as the rate constants are varied as would be expected when one metal ion is substituted for another, the simulated isotope effects and V_{max}'s change exactly as the experimental ones do. The value of V_{max} when Mg^{2+} is present is largest, while V_{max} for Ni^{2+} and V_{max} for Ca^{2+} are similar but smaller than that for Mg^{2+}. ^{D}V is smallest when Ca^{2+} is present and is larger for Mg^{2+} and Ni^{2+}. If the restriction requiring rate constants to reflect to some extent ligand exchange rates is not strictly adhered to (since the values of these constants may be more similar to one another on the enzyme than in solution), the observed results (^{D}V and V_{max}) are just as readily simulated, with the simulated results just as closely mirroring the observed values.

Some of the ^{D}V values in the Ca^{2+} column are <1.0, indicating an inverse isotope effect. Since the simulated values cannot be taken as absolute but can only predict trends, this is not an inconsistency. As ^{D}V approaches 1.0, C_r (the reverse commitment to catalysis) approaches $-^{D}k/(^{D}K_{eq} - 1.0)$. So, this is just a result of C_r changing beyond $-^{D}k/(^{D}K_{eq} - 1.0)$.

Some of the results in Table VI are shown to illustrate the effect of changing ratios of rate constants, or absolute values of rate constants, on the calculated values of ^{D}V and V_{max}. For instance, rows 1 and 2 under Mg^{2+} illustrate the effect of decreasing k_{13} and k_{14} while the ratio k_{13}/k_{14} is constant. As shown, both V_{max} and ^{D}V decrease. In rows 2 and 3 under Ni^{2+}, k_9 and k_{10} are changed while the ratio k_9/k_{10} is held constant. In this case, V_{max} decreases as the rate constants decrease, but ^{D}V increases. Rows 1 and 2 under Ca^{2+} and rows 3 and 4 under Ni^{2+} show that when both the rate constants and their ratios are changed, more complex behavior results. More examples of the effects of changing rate constants and their ratios can be seen in rows 4–6.

$^{D}V/K$ values calculated for each set of rate constants in Table VI range from 1.0 to 1.36. These are limiting values at low concentration of the second substrate. Of course, the values calculated at infinite concentration of the second substrate were 1.0. As shown in Table II, the values of ^{D}v at low concentration of metal–ATP appear to approach a limiting value of approximately 1.2. So, the experimental values tend to approach the simulated limting values. As with the experimental ^{D}v values at low substrate concentration, $^{D}V/K$ values showed no dependence on the identity of the metal ion present.

Discussion

The results presented herein can best be interpreted by referring to the model presented in Figure 4. As shown in Figure 4, the first two catalytic steps involve binding of substrates, H_2O and γ-monodentate metal–ATP. These may bind in an ordered fashion or randomly, to produce complex 1, or the H_2O molecule may be brought in by the metal ion. That F_1 initially binds the γ-monodentate metal–ATP complex as the substrate for the hydrolysis reaction is indicated by several recent studies (Gruys et al., 1985; Bossard & Schuster, 1981; Bossard et al., 1982). Monodentate complexes as substrates or products have been proposed for other enzymes (Dunaway-Mariano & Cleland, 1980b). Physiologically this may be important because in the direction of net ATP synthesis, less product inhibition would result if the product were γ-monodentate ATP because the β,γ-bidentate complex predominates in solution (Dunaway-Mariano & Cleland, 1980b). It should be noted that in no way does the mechanism in Figure 4 attempt to describe the specific interactions of the metal ion, the nucleotide(s), or the metal–nucleotide complex(es) with the enzyme. Metal ions, including the catalytic metal ion, bind directly to the enzyme, as do the catalytic nucleotide and the metal–nucleotide complexes. The mechanism in Figure 4 does not attempt to portray these interactions. So, all metal ion ligands other than nucleotide phosphate oxygens are simply represented by H_2O molecules, and no ligands to phosphate oxygens or charges on these oxygens are presented.

Complex 3 in Figure 4 is an F_1-bound P_i–metal–ADP intermediate. The existence of this intermediate has previously been proposed and supported (Gruys et al., 1985; Bossard ete al., 1980; Cross, 1981). Thus, in order to be consistent with a γ-monodentate substrate and a P_i–metal–ADP intermediate, the enzyme must catalyze the formation of a β,γ-bidentate metal–ATP complex which then undergoes hydrolysis (or must catalyze metal chelation to the β-phosphate concomitantly with hydrolysis). Such a shift in coordination of phosphate ligands along a polyphosphate chain has been proposed for other enzymes, especially kinases (Gupta & Mildvan, 1977; Mildvan, 1979; Dunaway-Mariano & Cleland, 1980b; Burgers & Eckstein, 1980; Tomasselli & Noda, 1983).

Examples of mono- to bidentate conversion of metal–ATP complexes (Bossard et al., 1982) and of interconversion of diastereomers of α,β-bidentate metal–ATP complexes (Gruys & Schuster, 1983) indicate these reactions are base-catalyzed. Once a proton is removed from a metal-coordinated water molecule, the hydroxyl group labilizes a replaceable oxygen ligand (H_2O for mono- to bidentate conversion) which may then be replaced by another oxygen ligand (a β-phosphate oxygen for mono- to bidentate conversion). It has been suggested (Bossard et al., 1982) that an active site base residue promotes this metal migration by initiating and facilitating the initial proton removal. Active site base residues have been proposed to function in similar capacities in phosphoryl transfer (Dunaway-Mariano & Cleland, 1980b) and other enzymes. An example is carbonic anhydrase and the active site Zn^{2+} involved (Cook et al., 1984). Deprotonation of a Zn^{2+}-bound water molecule is enzymatically facilitated and is rate-determining (Tu & Silverman, 1986). The binding energy of the hydroxyl is therefore increased, but that of the remaining water molecules is decreased. Nucleophilic attack on the metal ion further decreases this H_2O bond energy, and a water molecule is replaced by the nucleophile. During F_1 catalysis this would correspond to nucleophilic attack of a β-phosphate oxygen of ATP on the catalytic metal ion after deprotonation of a metal-bound water molecule, with concomitant loss of a water molecule from the metal ion coordination sphere (step k_9/k_{10} in Figure 4). Thus, the metal ion migrates along the nucleotide polyphosphate chain.

Hammes and Levison (1964) proposed that rate regulation of enzyme-catalyzed reactions involving divalent cations would be related to the acidity of the metal ion (pK_a of the H_2O molecules in the primary coordination sphere) and to the association–dissociation of metal–nucleotide complexes (K_{stab}). An example is pyruvate kinase catalysis where the rate of enolization of pyruvate depends on the pK_a of the water coordinated to the nucleotide-bound divalent metal ion (Robinson & Rose, 1972; Gupta et al., 1976). Metal ions with extreme

values of these constants would be poor activators while those with more intermediate values would be better activators.

If this were the case for F_1, a plot of V_{max} vs. pK_a (of metal-coordinated water molecules) or K_{stab} (of metal–nucleotide complexes) should show a peak at intermediate values of pK_a or K_{stab}. Figure 1 shows this to be the case. Interestingly, similar relationships can be shown for other enzymes. If the velocities (ATPase activities) of the 13S coupling factor of oxidative phosphorylation from *Alcaligenes faecalis* are ploted vs. the pK_a of the metal ion present, a smooth curve results with an optimum around the pK_a of Mg^{2+} (Adolfsen & Moudrianakis, 1978). The point for Fe^{2+} is not on the curve; however, no precautions were taken apparently to maintain this ion in the 2+ oxidation state in solution. Another example is creatine kinase (Burgers & Eckstein, 1980). Again, a plot of velocity vs. pK_a of the metal present results in a smooth curve with an optimum around the pK_a of Mn^{2+}. As opposed to the study with beef heart F_1 presented here, the velocities in these latter two studies were not obtained by extrapolation to infinite substrate concentration.

Step k_9/k_{10} in Figure 4 is initiated by proton removal from a water molecule coordinated to the catalytic metal ion in the γ-monodentate metal–ATP complex and thus is regulated by the pK_a of that H_2O molecule. Step k_{13}/k_{14} is the equilibrium describing the association between ADP and the metal ion and is regulated by the particular metal–ADP stability constant. So, step k_9/k_{10} is more limiting for overall hydrolysis when the pK_a of the metal-bound water is large, and k_{13}/k_{14} is more limiting when the metal–ADP K_{stab} is large.

That the metal–ADP bond is broke before ADP is released is indicated by the results of Table IV, which show ADP inhibition is independent of the metal ion present. This is supported by the results of Hilborn and Hammes (1973) which show ADP binding to the catalytic site is independent of the presence of metal ion. Another recent study (Gruys et al., 1985) has shown that when Cd–ATPβS is the substrate for F_1-catalyzed hydrolysis, the reaction is predominantly limited by breaking of the Cd–S bond in a P_i–metal–ADPβS intermediate (Cd^{2+} chelated to P_i and to the β-phosphate of ADPβS through sulfur). So, since K_{stab} is different for each metal–ADP complex, the F_1-catalyzed rate would be more limited by k_{13}/k_{14} (Figure 4) when the metal–ADP complex stability constant is large.

The results of Dorgan et al. (1984) show that when divalent metal ions such as Ni^{2+} or Ca^{2+}, those with either very high metal–nucleotide stability constants or metal-coordinated water pK_a values, are present during F_1-catalyzed ATP hydrolysis, Arrhenius plots of data show straight lines. This indicates that the metal-dependent parameters are responsible for rate regulation and that when either the pK_a or K_{stab} becomes very large, the reaction becomes more limited by a single step. The results in Figure 1 show that V_{max} for F_1-catalyzed ATP hydrolysis is smallest when the metal ion present is characterized by a high of pK_a of its coordinated H_2O molecules or a large metal–nucleotide stability constant. As temperature is changed, a prediction can be made as to how the curve should change based on the variation of the metal ion properties with temperature and how these properties affect the reaction rate. As temperature is increased, the metal ions all become more acidic (Burgess, 1978), and the rate constants characterizing the entire reaction increase, so unsurprisingly the rate of the reaction should increase regardless of the metal ion present. However, the results of Taqui Khan and Martell (1967) show that an increase in temperature causes the ADP stability constant with Mg^{2+} to increase, while those with Mn^{2+}, Ni^{2+}, and Ca^{2+} decrease. So, as temperature is raised, it would be expected that the peak of the curve in Figure 1 should shift toward higher initial values of K_{stab} or lower initial pK_a values. This is indeed what happens, as is seen in Figure 2. Since the Mn–ADP stability constant decreases, the rate of Mn–ATP hydrolysis increases faster with temperature than the rate with Mg^{2+}, so the peak of the curve shifts toward Mn^{2+}. As shown, the Cd^{2+} rate increases even faster than that with Mn^{2+} as temperature increases. Unfortunately, it is not known how K_{stab} for Cd–ADP varies with temperature. Since in the 12–40 °C range studied by Taqui Khan and Martell (1966, 1967) the adenosine nucleotide constants with Mg^{2+} are the only ones that increased as temperature increased, the Cd–ADP constant probably decreases like the others. So this evidence and all the preceding evidence clearly and strongly indicate that the metal–ADP bond is broken before ADP release and that this step is at least somewhat rate determining.

Interestingly, from Figure 1 it can be seen that the point corresponding to F_1-catalyzed Zn–ATP hydrolysis does not fit on the curve of V_{max} vs. pK_a but does fit on the curve of V_{max} vs. the K_{stab} of the metal–ADP stability constant. That the point for Zn^{2+} fits on the latter curve is exactly as would be expected if the rate of Zn–ATP hydrolysis were limited more by the breaking of the Zn–ADP bond (since K_{stab} is large) than by the pK_a of Zn^{2+}-coordinated H_2O molecules. Why the pK_a of Zn^{2+} and the Zn–ADP stability are not related to each other as these constants appear to be for the other metal ions tested is not clear. However, this is again more evidence that the metal–ADP bond is broken before ADP is released.

Proton removal from a metal-coordinated water molecule by an enzymic base residue would be an isotopically sensitive step during F_1 catalysis (step k_9/k_{10} in Figure 4). As with the effect of temperature, the differences in the observed isotope effects when different metal ions are present must be a result of the differences in the properties of the metal ions responsible for regulation of the catalytic reaction. So, when one metal ion is replaced by another, the rate constants in both steps k_9/k_{10} and k_{13}/k_{14} change, and these changes must account for the resulting differences in the isotope effects observed. Since the K_{stab} and pK_a values for these metal ions and complexes are known, the rate constants and equilibrium constants of steps k_9/k_{10} and k_{13}/k_{14} can be varied systematically to correspond to a specific metal ion. In this way, the isotope effects can be simulated and the results of the simulations compared to the observed data.

The results of the simulations in Table VI are consistent with the observed results of Table II. As k_9/k_{10} is raised (pK_a of a metal-coordinated water molecule is raised) with a concomitant decrease in k_{13}/k_{14} (metal–nucleotide stability constant is decreased), ^DV decreases. This is equivalent to changing the metal ion during F_1-catalyzed metal–ATP hydrolysis from Ni^{2+} to Mg^{2+} to Ca^{2+}. Also, the simulated V_{max} values change as the experimental ones do; V_{max} when Mg^{2+} is present is larger than V_{max} when either Ni^{2+} or Ca^{2+} are present, the values for the latter two being roughly equivalent. Obviously, the simulated V_{max} values must change as the experimental ones do as one metal ion is substituted for another. So, the experimental isotope effects (and V_{max} values) change as the metal ion is changed as they would be expected to according to how the acidity of the metal ion and metal–nucleotide stability constants vary from one metal ion to another, within the mechanistic bounds of Figure 4.

The mechanism in Figure 4 shows substrate binding to be ordered. Changing the order does not affect the calculated

(simulated) values of V_{max} or ^{D}V. For a random substrate binding mechanism, these values are not changed either. However, the values of $^{D}V/K$ do change when the order of substrate binding is changed or randomized.

As mentioned above (see Results), values of $^{D}V/K$ were also simulated. For the cases shown in Table VI, the values ranged from 1.0 to 1.36 (limiting values) for the ordered mechanism, with metal–ATP binding last. If metal–ATP binds first, the ratio k_5/k_4 decreases, C_f decreases, and $^{D}V/K$ increases. The limiting values of $^{D}V/K$ in a random mechanism are also higher in this instance. Statistically significant values of $^{D}V/K$ (extrapolated) could not be obtained (see Results). However, as substrate concentration decreased, ^{D}v approached a value of 1.2 regardless of the metal ion present. This is consistent with the simulated results (above) in that all limiting values of $^{D}V/K$ were similar regardless of the metal ion present, for an ordered mechanism. However, the simulated values of $^{D}V/K$ for a random mechanism are much higher for situations in Table VI corresponding to Mg^{2+} and Ni^{2+} than for Ca^{2+}, as they are for an ordered mechanism with metal–ATP binding first. So, the results are more consistent with an ordered addition of substrate binding during the hydrolysis reaction, with metal–ATP binding last.

Figure 4 depicts product release as ordered with ADP released first. Since both steps are reversible, changing the order does not affect ^{D}V. $^{D}V/K$ would be affected if k_{15} and k_{17} were different, but the trends that occur as one metal ion is substituted for another would not change. However, if the P_i dissociation rate changes significantly depending on the metal io present, ^{D}V and $^{D}V/K$ will be subject to these changes (this would only affect $^{D}V/K$ if P_i is released first from the enzyme). However, this is not likely since the binding of P_i to the enzyme is so poor during catalysis. Product release order is further addressed below.

Catalytic deprotonation of the metal-bound water molecule would require a basic residue on the enzyme. If the basicity of this residue is perturbed, then a "perturbation effect" will be observed for the reaction, analogous to an isotope effect. An active site tyrosine on F_1 is susceptible to nitration by tetranitromethane, which greatly inhibits activity (Senior, 1973). An active site tyrosine is also modified by NBD-Cl (Ferguson et al., 1976). The work of Lunardi et al. (1979) and Dorgan and Schuster (1981) showed nitration by tetranitromethane affected the binding of nucleotides to F_1. The results of Esch and Allison (1978) suggested this tyrosine acts as an acid–base catalyst and is directly involved in catalysis. One study places an active site tyrosine near the γ-phosphate of ATP (Ting & Wang, 1980).

Nitration of a tyrosine ortho to the phenolic group (Sololovsky et al., 1966) lowers the pK_a significantly (from 10 to about 7; Riordan & Vallee, 1972), rendering the tyrosine less efficient as a base. If the tyrosine were responsible for a catalytic deprotonation, then nitration of a tyrosine would cause a "nitration effect" to be observed, much the same as an isotope effect.

Divalent metal ions are generally less acidic in D_2O solution than in H_2O [$K_a(H_2O)/K_a(D_2O) > 1.0$; Burgess, 1978]. This trend is also observed in the isotope effect on the equilibrium constant ($^{D}K_{eq}$) for transfer of a proton from H_3O^+ to ROH. In this case, the value of $^{D}K_{eq} = 0.33$ [$[k_f(H_2O)/k_f(D_2O)]/[k_r(H_2O)/k_r(D_2O)]$; Schowen, 1977]. If ^{D}k [$k_f(H_2O)/k_f(D_2O)$] = 5, and $^{D}K_{eq} = 0.33$, then $^{D}k_r$ is approximately 14. So, in the case of isotope effects on F_1, $^{D}k_r$ is greater than $^{D}k_f$. Then for these isotope effects, $k_f(H_2O) > k_f(D_2O)$, and $k_r(H_2O) > k_r(D_2O)$, with the former ratio smaller than the latter as mentioned above. However, for a nitration effect, $k_r(U)/k_f(N)$ is still >1, but since the nitrated enzymic base is more acidic, $k_r(U)/k_r(N) < 1.0$. So not only would $^{N}K_{eq}$ be >1.0, but it would also be $>{}^{N}k_f$.

If $^{D}K_{eq}(1 + R_f/E_f) < {}^{D}K + R_f/E_f$, then as C_r increases, ^{D}V decreases. This is the case for the simulated values in Table VI (since all values of R_f/E_f are between 2 and 7). C_r is larger for the results in the Ca^{2+} column, smallest in the Ni^{2+} column and intermediate for Mg^{2+}. So ^{D}V is greatest for Ni^{2+} and smallest for Ca^{2+} (even though R_f/E_f values are different, they are within a factor of <5, so these differences cause minimal perturbation). However, for a nitration effect, $^{N}K_{eq} > {}^{N}k$ (as shown above), and $^{N}K_{eq}(1 + R_f/E_f) > {}^{N}k + R_f/E_f$. So in this case, whereas ^{D}V decreases as C_r increases, ^{N}V increases as C_r increases. In other words, a nitration effect on F_1-catalyzed metal–ATP hydrolysis should be greatest if Ca^{2+} is the metal cation present and smallest when Ni^{2+} is present. This is exactly what is observed in Table III. ^{N}V when Ca^{2+} is present is greatest (approximately 2) while ^{N}V when Ni^{2+} is present is almost 1.0. These results are precisely what would be expected on the basis of the differing perturbing effects of D_2O and nitration, as one metal ion is substituted for another on the basis of the aforementioned metal ion properties.

In contrast to ADP inhibition, P_i inhibition of F_1-catalyzed ATPase activity is clearly dependent on the metal ion present (see Table V) at both high and low temperature. This indicates that, during catalysis, P_i binding to the catalytic site is dependent on the presence of a metal ion and is subject to the properties of that metal ion. The results of Penefsky (1977) show a metal requirement of P_i binding to beef heart F_1, which was suggested to be absolute. It was also suggested that the interaction occurred between an enzyme-bound metal and free P_i. These suggestions were supported by results of spinach chloroplast coupling factor (CF_1) studies which indicate that a ternary complex, enzyme–metal–P_i, was formed at a catalytic site, through binding of P_i to an enzyme–metal complex (Younis et al., 1983). Studies with the carboxyl group modifier DCCD (dicyclohexylcarbodiimide) also support these suggestions. This compound modifies catalytic site glutamate residues which are the metal binding sites (Yoshida et al., 1982). Mg^{2+} protects against this modification. P_i enhances the Mg^{2+} protection but does not provide protection itself. This also suggests that a ternary enzyme–metal–P_i complex is formed.

As seen in Table V, P_i inhibition becomes increasingly noncompetitive as temperature is raised. Since ADP inhibition is competitive, these results suggest that as the temperature is increased, the order of release of ADP and P_i shifts toward P_i being released first. The results of Schuster et al. (1976) indicate that, during ATP synthesis catalyzed by F_1, P_i binds to the enzyme before ADP. This suggests ADP is released before P_i during hydrolysis. The results of Grubmeyer et al. (1982) show that P_i increases the rate of ADP binding but not the ADP dissociation rate. So, K_{eq} for ADP dissociation is smaller in the presence of P_i. Also, their results indicate that the rate constant for P_i release is greater than that for ADP release and are interpreted to suggest P_i is released first during hydrolysis. However, their experiments were performed under "uni-site" conditions. In any case, it is clear that the question of order or lack of order of substrate binding and product release has not been fully answered, especially considering the apparent temperature dependence.

The results in Figure 3 show that negative cooperativity occurs when Ni^{2+} is the divalent metal ion present during F_1-catalyzed ATP hydrolysis. Negative cooperativity with

Mg^{2+} present is well established (Ebel & Lardy, 1975) and occurred under the conditions of these experiments (results not shown). Interestingly, positive cooperativity occurs when Ca^{2+} is present (Figure 3). In skeletal muscle A particles, the concentration of Ca^{2+} regulates the dimerization of F_1I (ATPase inhibitor protein), the dimer being the active form (Yamada et al., 1981). It has also been demonstrated that Ca^{2+} binds to a tight metal binding site on F_1 differently than other divalent metal ions (Daggett et al., 1985). These observations indicate that Ca^{2+} plays an active role in the catalytic and regulatory aspects of F_1-catalyzed reactions, which may be important physiologically. Catalytically, it is not readily apparent how Ca^{2+} causes positive cooperativity to occur. It is also not readily evident how positive cooperativity could be incorporated into the regulatory scheme of the most promoted mechanism of F_1 function, the binding change mechanism (Gresser et al., 1982).

The results of the metal ion studies presented herein and the results of the other studies mentioned above suggest the catalytic mechanism shown in Figure 4. F_1 initially binds a γ-monodentate metal–ATP complex as substrate. An active site tyrosinate ion is then involved in deprotonation of a metal-bound H_2O molecule, which leads to nucleophilic attack by a β-phosphate oxygen on the metal ion. In this way, a β,γ-bidentate metal–ATP complex may be formed before hydrolysis, or hydrolysis may occur concomitantly with metal ion chelation to the β-phosphate. In either case, a P_i–metal–ADP intermediate is formed. The metal–ADP bond is then broken before product release.

ACKNOWLEDGMENTS

We thank Dr. David N. Silverman for a copy of his manuscript prior to publication.

REFERENCES

Adolfsen, R., & Moudrianakis, E. N. (1978) *J. Biol. Chem. 253*, 4380–4388.

Amzel, L. M., & Pedersen, P. L. (1983) *Annu. Rev. Biochem. 52*, 801–824.

Baes, C. F., & Mesmer, R. E. (1976) *The Hydrolysis of Cations*, Chapters 5, 10, 12, and 13, Wiley, New York.

Basolo, F., & Pearson, R. G. (1967) *Mechanisms of Inorganic Reactions*, pp 52–123, Wiley, New York.

Bossard, M. J., & Schuster, S. M. (1981) *J. Biol. Chem. 256*, 6617–6622.

Bossard, M. J., Vik, T. A., & Schuster, S. M. (1980) *J. Biol. Chem. 255*, 5342–5346.

Bossard, M. J., Samuelson, G. S., & Schuster, S. M (1982) *J. Inorg. Biochem. 17*, 61–68.

Bradford, M. (1976) *Anal. Biochem. 72*, 246–256.

Burgers, P. M. J., & Eckstein, F. (1980) *J. Biol. Chem. 255*, 8229–8233.

Burgess, J. (1978) in *Metal Ions in Solution*, Chapter 9, Horwood, Sussex.

Cleland, W. W. (1967) *Adv. Enzymol. Relat. Areas Mol. Biol. 29*, 1–32.

Cleland, W. W. (1982) *CRC Crit. Rev. Biochem. 13*, 385–428.

Cook, C. M.; Haydock, K., Lee, R. H. & Allen, L. C. (1984) *J. Phys. Chem. 88*, 4875–4880.

Cross, R. L. (1981) *Annu. Rev. Biochem. 50*, 681–714.

Daggett, S. G., Gruys, K. J. & Schuster, S. M. (1985) *J. Biol. Chem. 260*, 6213–6218.

Diebler, H., Eigen, M., & Hammes, G. G. (1960) *Z. Naturforsch., B: Anorg. Chem., Org. Chem., Biochem., Biophys., Biol. 15B*, 554–560.

Dorgan, L. J., & Schuster, S. M. (1981) *J. Biol. Chem. 256*, 3910–3916.

Dorgan, L. J., Urbauer, J. L., & Schuster, S. M. (1984) *J. Biol. Chem. 259*, 2816–2821.

Draper, N. R., & Smith, H. (1966) *Applied Regression Analysis*, Chapters 2, 4, and 10, Wiley, New York.

Dunaway-Mariano, D. D., & Cleland, W. W. (1980a) *Biochemistry 19*, 1496–1505.

Dunaway-Mariano, D. D., & Cleland, W. W. (1980b) *Biochemistry 19*, 1506–1515.

Ebel, R. E., & Lardy, H. A. (1975) *J. Biol. Chem. 250*, 191–196.

Eigen, M., & Hammes, G. G. (1960) *J. Am. Chem. Soc. 82*, 5951–5952.

Eigen, M., & Hammes, G. G. (1961) *J. Am. Chem. Soc. 83*, 2786.

Esch, F. S., & Allison, W. S. (1978) *J. Biol. Chem. 253*, 6100–6106.

Esch, F. S., Bohlen, P., Otsuka, A. S., Yoshida, M., & Allison, W. S. (1981) *J. Biol. Chem. 256*, 9084–9089.

Ferguson, S. J., Lloyd, W. J., Lyons, M. H. & Radda, G. D. (1975) *Eur. J. Biochem. 54*, 117–126.

Fletcher, R., & Powell, M. J. D. (1963) *Comput. J. 6*, 163–168.

Gresser, M. J., Meyers, J. A., & Boyer, P. D. (1982) *J. Biol. Chem. 257*, 12030–12038.

Grubmeyer, C., Cross, R. L., & Penefsky, H. S. (1982) *J. Biol. Chem. 257*, 12092–12100.

Gruys, K. J., Urbauer, J. L., & Schuster, S. M. (1985) *J. Biol. Chem. 260*, 6533–6540.

Gupta, R. K., & Mildvan, A. S. (1977) *J. Biol. Chem. 252*, 5967–5976.

Gupta, R. K., Oesterling, R. M., & Mildvan, A. S. (1976) *Biochemistry 15*, 2881–2887.

Hammes, G. G., & Levison, S. A. (1964) *Biochemistry 3*, 1504–1506.

Heinonen, J. K., & Lahti, R. J. (1981) *Anal. Biochem. 113*, 313–317.

Hilborn, D. A., & Hammes, G. G. (1973) *Biochemistry 12*, 983–990.

Knowles, A. F., & Penefsky, H. S. (1972) *J. Biol. Chem. 247*, 6617–6623.

Layne, E. (1957) *Methods Enzymol.* 3, 447–454.

Lowry, D. H., Rosebrough, N. J., Farr, A. L., & Randall, R. J. (1951) *J. Biol. Chem. 193*, 265–275.

Lunardi, J., Satre, M., Bof, M., & Vignais, P. V. (1979) *Biochemistry 18*, 5310–5316.

Mildvan, A. S. (1979) *Adv. Enzymol. Relat. Areas Mol. Biol. 49*, 103–126.

Northrop, D. B. (1981a) *Biochemistry 20*, 4056–4061.

Northrop, D. B. (1981b) *Annu. Rev. Biochem. 50*, 103–131.

Northrop, D. B. (1982) *Methods Enzymol. 87*, 607–625.

Pedersen, P. L. (1975) *J. Bioenerg. 6*, 243–275.

Pedersen, P. L. (1982) *Ann. N.Y. Acad. Sci. 402*, 1–20.

Pedersen, P. L., LeVine, H., III, & Cintron, N. (1974) in *Membrane Proteins in Transport and Phosphorylation*, pp 43–54, North-Holland, Amsterdan.

Penefsky, H. S. (1977) *J. Biol. Chem. 252*, 2891–2899.

Petersen, G. L. (1978) *Anal. Biochem. 84*, 164–172.

Pougeois, R., Satre, M., & Vignais, P. V. (1979) *Biochemistry 18*, 1408–1413.

Pullman, M. E., Penefsky, H. S., Datta, A., & Racker, E. (1960) *J. Biol. Chem. 235*, 3322–3329.

Riordan, J. F., & Vallee, B. L. (1972) *Methods Enzymol. 25*, 515–521.

Riordan, J. F., Sokolovsky, M., & Vallee, B. L. (1967) *Biochemistry 6*, 3609–3617.

Robinson, J. L., & Rose, I. A. (1972) *J. Biol. Chem. 247*, 1096-1105.
Salomaa, P., Schaleger, L. L., & Long, F. A. (1964) *J. Am. Chem. Soc. 86*, 1-7.
Schendel, P. R., & Wells, R. D. (1973) *J. Biol. Chem. 248*, 8319-8321.
Schowen, K. B., & Schowen, R. L. (1982) *Methods Enzymol. 87*, 551-606.
Schowen, R. L. (1977) in *Isotope Effects on Enzyme-Catalyzed Reactions*, pp 64-99, University Park Press, Baltimore.
Schuster, S. M., Reinhart, G. D., & Lardy, H. A. (1977) *J. Biol. Chem. 252*, 427-432.
Selwyn, M. J. (1967) *Biochem. J. 105*, 279-288.
Selwyn, M. J. (1968) *Nature (London) 219*, 490-493.
Senior, A. E. (1973) *Biochemistry 12*, 3622-3627.
Sololovsky, M., Riordan, J. R., & Vallee, B. L. (1966) *Biochemistry 5*, 3582-3589.
Spitsberg, V. L., & Blair, J. E. (1977) *Biochim. Biophys. Acta 460*, 136-141.
Taqui Kahn, M. M., & Martell, A. E. (1966) *J. Am. Chem. Soc. 88*, 668-671.
Taqui Kahn, M. M., & Martell, A. E. (1967) *J. Am. Chem. Soc. 89*, 5586-5590.
Ting, L. P., & Wang, J. H. (1980) Biochemistry *19*, 5665-5670
Tomasselli, A. B., & Noda, L. H. (1983) *Eur. J. Biochem. 132*, 109-115.
Tu, C. K., & Silverman, D. N. (1986) *J. Am. Chem. Soc. 108*, 6065-6066.
Wang, J. H. (1983) *Annu. Rev. Biophys. Bioeng. 12*, 21-34.
Yamada, E. W., Huzel, N. J., & Diekisen, J. C. (1981) *J. Biol. Chem. 256*, 10203-10207.
Yoshida, M., Poser, J. W., Allison, W. S., & Esch, F. S. (1981) *J. Biol. Chem. 256*, 148-153.
Yoshida, M., Allison, W. S., Esch, F., & Futai, M. (1982) *J. Biol. Chem. 257*, 10033-10037.
Younis, H. M., Weber, G., & Boyer, J. S. (1983) *Biochemistry 22*, 2505-2512.

DNA-Dependent Adenosinetriphosphatase B from Mouse FM3A Cells Has DNA Helicase Activity†

Masayuki Seki,* Takemi Enomoto, Fumio Hanaoka, and Masa-atsu Yamada
Department of Physiological Chemistry, Faculty of Pharmaceutical Sciences, University of Tokyo, 7-3-1 Hongo, Bunkyo-ku, Tokyo 113, Japan

Received October 7, 1986; Revised Manuscript Received January 7, 1987

ABSTRACT: We have detected at least four forms of DNA-dependent ATPase in mouse FM3A cell extracts [Tawaragi, Y., Enomoto, T., Watanabe, Y., Hanaoka, F., & Yamada, M. (1984) *Biochemistry 23*, 529-533]. The purified fraction of one of the four forms, ATPase B, has been shown to have DNA helicase activity by using a DNA substrate which permits the detection of limited unwinding of the helix. The DNA substrate consists of single-stranded circular *fd* DNA and the hexadecamer complementary to the *fd* DNA, which bears an oligo(dT) tail at the 3′ terminus. The helicase activity and DNA-dependent ATPase activity cosedimented at 5.5 S on glycerol gradient centrifugation. The helicase required a divalent cation for activity ($Mg^{2+} \simeq Mn^{2+} > Ca^{2+}$). The optimal concentrations of these divalent cations were 5 mM. The requirement of divalent cations of the DNA helicase activity was very similar to that for the DNA-dependent ATPase activity of ATPase B. The helicase activity was absolutely dependent on the presence of a nucleoside triphosphate. ATP was the most effective cofactor among the ribo- and deoxyribonucleoside triphosphates tested, and considerable levels of helicase activity were observed with other ribo- and deoxyribonucleoside triphosphates. The efficiency of a nucleoside triphosphate to serve as cofactor for the helicase activity correlated with the capacity of the nucleotide to serve as substrate for the DNA-dependent ATPase activity. The nonhydrolyzable ATP analogues such as adenosine 5′-*O*-(3-thiotriphosphate) were not effective for the helicase activity. The helicase displaced the hexadecamer with no tail as well as the hexadecamer bearing the 3′ or 5′ tail. The efficiency of displacement was almost the same among the three substrates.

On the replication of duplex DNA, DNA helicase action is required for unwinding the double strand in advance of a replication fork. It has been indicated that the bacteriophage T7 gene *4* protein, the T4 gene *41* protein, and the *Escherichia coli rep* protein are required for the replication of the chromosome of coliphages T7, T4, and *φX174* RF, respectively (Kornberg, 1980). The *E. coli dnaB* protein is also essential for the replication of oriC plasmid containing the replication origin of *E. coli* chromosome (Ogawa et al., 1985). Biochemical analysis of these proteins in vitro has indicated that they have DNA helicase activity and this activity is coupled with hydrolysis of nucleoside 5′-triphosphate in a DNA-dependent manner (Kornberg, 1980; Yarranton & Gefter, 1979; Venkatesan et al., 1982; Matson et al., 1983; LeBowitz & McMacken, 1986).

To find analogous proteins participating in eukaryotic DNA replication, eukaryotic DNA-dependent ATPases have been isolated from various sources (Hachmann & Lezius, 1976; Otto, 1977; Hotta & Stern, 1978; Cobianchi et al., 1979; Assairi & Johnston, 1979; Boxer & Korn, 1980; Plevani et al., 1980; Dejong et al., 1981; Hyodo & Suzuki, 1981; Yaginuma & Koike, 1981; Thomas & Meyer, 1982; Brewer et al.,

† This work was supported in part by Grants-in-Aid for Scientific Research and for Cancer Research from the Ministry of Education, Science, and Culture of Japan and by the Naito Foundation.

0006-2960/87/0426-2924$01.50/0